Influence of Ti layer thickness on solid state amorphization and magnetic properties of annealed Ti/Ni multilayer

2007 J. Phys.: Condens. Matter 19 376210

(http://iopscience.iop.org/0953-8984/19/37/376210)

IOP PUBLISHING JOURNAL OF PHYSICS: CONDENSED MATTER

J. Phys.: Condens. Matter **19** (2007) 376210 (11pp) doi:10.1088/0953-8984/19/37/376210

Influence of Ti layer thickness on solid state amorphization and magnetic properties of annealed Ti/Ni multilayer

Pramod Bhatt[1,2,3], **S M Chaudhari**[2,4] **and M Fahlman**[1]

[1] Department of Science and Technology, Linköping University, SE-601 74 Norrköping, Sweden
[2] UGC-DAE Consortium for Scientific Research, University Campus, Khandwa Road, Indore-452017, MP, India

E-mail: prabh@itn.liu.se

Received 6 March 2007, in final form 27 July 2007
Published 22 August 2007
Online at stacks.iop.org/JPhysCM/19/376210

Abstract

Annealing induced SSR (solid state reaction) leading to amorphization and magnetic properties as a function of Ti layer thickness has been investigated using XRD (x-ray diffraction), GIXRR (grazing incidence x-ray reflectivity) and MOKE (magneto-optical Kerr effect) measurements. [Ti(t Å)/Ni(50 Å)] $\times$10 ML samples where t = 30, 50 and 70 Å have been prepared by using electron beam evaporation technique under ultra-high vacuum conditions at room temperature. The amorphization process was carefully studied using XRD and GIXRR techniques showing that the SSA (solid state amorphization) temperature gradually decreases with increasing Ti layer thickness. Corresponding MOKE measurements show a magnetic to non-magnetic transition near the amorphization temperature (T_A) with annealing, for each of the Ti layer thicknesses, due to crystalline Ti–Ni alloy phase formation at interfaces. The saturation magnetization and coercivity were also modified with Ti layer thickness variation. In addition to this, anisotropy developed with Ti layer thickness and diminished with increasing annealing temperatures. All these magnetic changes due to Ti layer thickness variations are interpreted in terms of amorphization and micro-structural changes near the SSA temperature.

(Some figures in this article are in colour only in the electronic version)

[3] Author to whom any correspondence should be addressed. Present address: Department of Science and Technology (ITN), Linköping University, SE-601 74 Norrköping, Sweden.
[4] Deceased.

1. Introduction

Study of multilayer structure has been one of the most exciting research fields for the last few years because of its promising technological applications. There are various technological applications where multilayer structure can be used; in particular, metallic magnetic multilayer and spin-valve structures already find many applications in magnetic heads and in magnetic hard disk drives, head tape devices, and various components in micro-electromechanical systems (MEMS) with very compact shape and size [1, 2]. It is well known that microstructure, surface morphology, electronic, magnetic and electrical properties of multilayer films are extremely sensitive to lattice strain and lattice mismatch between substrate and film, and of course these effects strongly depend on the film thickness [3–5]. Therefore, the thickness effect in a multilayer system can not be ignored, especially in terms of magnetic properties, as seen from recent published literature on the thickness effect [6–9]. Generally, for any kind of MLS, individual layer thickness is a crucial parameter, which could lead to an increase in surface roughness, and concurrently increased light scattering results in a change in the corresponding electronic, magnetic and structural properties. Recently, the thickness effect on a shape memory Ti–Ni alloy thin film has been investigated by Ishida *et al*, and they found that the transformation strain and residual strain under a constant stress are very sensitive to the film thickness when the layer thickness is less than the average grain size [10]. The objective of the present work is, therefore, to understand the thickness effect on the atomic level mechanism of amorphization, the nature of their short-range order and the corresponding changes in magnetic properties of the multilayer system. The amorphization with layer thickness variation has also been interpreted in terms of the molecular dynamics model of amorphization.

The topic of amorphous alloy phase formation in multilayer systems is of great current interest, and a large number of works has been reported in reputable journals in recent years [11–14]. SSA in a ML (multilayer) system was first observed by Schwarz and Johnson in the Au–La system in 1983, which can be defined simply as a crystalline to amorphous phase transformation [15–17], induced by a variety of processes such as mechanical deformation, energetic particle irradiation or bombardment, and interface diffusion reactions. However, amorphization reactions are found to occur in systems where there is a large difference in atomic size between the component elements, and one element preferentially diffuses into the other. In this respect, the Ti/Ni ML has been considered as a model object for investigation of SSR which satisfies all necessary conditions for occurrence of SSR [18, 19]. These conditions are (i) large and negative heat of mixing, (ii) an anomalous diffusion of Ni in Ti and (iii) low mobility for one of the elements in the amorphous phase. Therefore, many experimental techniques have usually been used to study SSR in Ti/Ni multilayered systems: differential scanning calorimetry [20], Auger electron spectroscopy, x-ray photoelectron spectroscopy [21, 22], a few magnetic methods [23–25] and, of course, the traditional direct methods, i.e. x-ray diffractometry and transmission electron microscopy [26]. On the basis of published work it seems that many researchers have studied its structural properties, extensible with thermal treatment. For instance, Clemens reported that in Ni/Ti multilayer SSA could take place upon annealing when the interfacial layers were in a disordered state, and also that the interfacial reaction was completely suppressed if coherent interfaces emerged [18, 19]. Vredenber *et al* examined polycrystalline Ni/single crystal Zr(112) diffusion couples: for this case, it was found that amorphization could only take place after a disordered interlayer had been formed by an ion beam at the interface [27]. These observations imply that a sharp interface may act as a nucleation barrier against interfacial reaction.

Surprisingly, few reports [21–25] are available on corresponding electronic and magnetic property investigations of Ti/Ni MLS, possibly because of the electronic structures of alloys

at interfaces, which are not fully understood, primarily due to their lack of periodicity, and fundamental questions such as how alloying affects the hybridization between neighboring atoms or how it changes the valence band density of states have not been yet answered. However, the fact is that Ni is ferromagnetic, so study of magnetic properties of this system can also bring additional information on the state of the interface.

2. Experimental details

[Ti(t Å)/Ni(50 Å)] $\times$10 multilayer samples, where t = 30, 50 and 70 Å, have been deposited on float glass substrate using the electron beam evaporation technique under UHV conditions at room temperature [28]. In order to avoid contamination during deposition, the system was thoroughly backed to a temperature up to 200 °C for 12 h to achieve a background pressure of 5×10^{-10} Torr. Deposition of both Ti and Ni layers was carried out at a rate of 0.1 Å s^{-1}. During deposition, the thickness of each layer was monitored using a water-cooled quartz crystal thickness monitor. Multilayer samples prepared in this way were annealed up to 500 °C with a step of 100/50 °C for 1 h under high vacuum of the order of 10^{-7} Torr. All measurements were carried out at room temperature after cooling down the samples after annealing. The layer thickness, surface and interface roughness and electron density have also been confirmed by using GIXRR *ex situ*. The structural characterizations of these ML samples were carried out using XRD and GIXRR techniques. A Rigaku diffractometer equipped with a shielded Cu tube as a source of x-rays having 18 kW power was employed for XRD measurements. The corresponding magnetization behavior of these multilayer samples with Ti layer thickness variations were studied by using surface sensitive MOKE technique. All the MOKE measurements were carried out at 6328 Å wavelength using a He–Ne laser source.

3. Results and discussion

Figure 1 shows the XRD patterns of as-deposited as well as annealed Ti/Ni multilayer samples up to 500 °C with Ti layer thickness of 30, 50 and 70 Å respectively, whereas the Ni layer thickness of 50 Å is constant for each multilayer. These figures are denoted as figures 1(a), (b) and (c) for ML samples A = [Ti(30 Å)/Ni(50 Å)] $\times$ 10, B = [Ti(50 Å)/Ni(50 Å)] $\times$ 10 and C = [Ti(70 Å)/Ni(50 Å)] $\times$ 10 respectively. The XRD pattern of the as-deposited case for all multilayer samples shows a strong peak at 44.5° corresponding to the Ni(111) reflection and the Ti(002) peak at 38.4° suggests a crystalline nature of the deposited films, especially for ML samples B and C. However ML sample A does not show any peak corresponding to the Ti(002) reflection in the XRD spectrum of the as-deposited case. Increasing Ti layer thickness, Ti(002) peak structure develops at 38.4° (see figure 1(b)) and is clearly visible for the multilayer sample having a Ti layer of 70 Å (see figure 1(c)). The reason for this is the amorphous nature of the 30 Å Ti layer, which is deposited in amorphous form at this thickness for multilayer sample A. Meanwhile, in the multilayer for higher Ti layer thickness of 30 Å, Ti is deposited mainly in crystalline HCP form, resulting in the appearance of the Ti(002) peak in XRD patterns of multilayers B and C. It is well established that below a certain critical layer thickness electron-beam deposited films are generally in amorphous in nature. Therefore, in the case of the ML with 30 Å Ti layer thicknesses, the long-range crystalline ordering may not be completed and the structure of the deposited layer results in an amorphous-like structure [29]. In addition to this, at the lower 2θ side of the Ni(111) peak, a small low intensity peak appears at 2θ values of 41.2°, which can be interpreted in terms of a Laue satellite, implying a practically constant Ni crystallite size in the direction perpendicular to the Ti–Ni interface in all Ti/Ni MLs [30, 31].

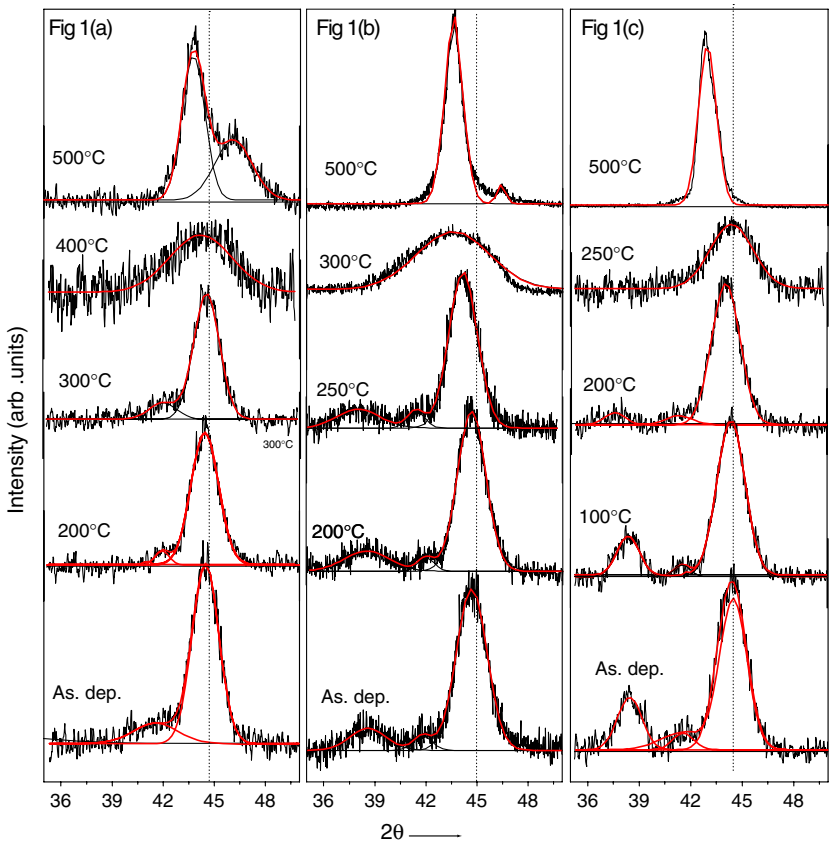

Figure 1. XRD patterns of Ti/Ni ML samples with Ti layer thickness variation as well as annealing temperatures. (a), (b), (c) correspond to multilayer samples having Ti layer thicknesses of 30, 50 and 70 Å respectively.

Slight reductions in peak intensities of Ti and Ni are found for ML samples annealed at 200 °C. Further annealing at 300 °C started to show some structural changes in the recorded XRD spectra, particularly for ML sample C. Ti and Ni peak intensities decrease and are found to be broad in this case.

Drastic changes are observed at an annealing temperature of 400 °C for multilayer sample A, where a broad hump at 43.2° instead of a crystalline Ni(111) peak is observed and suggests an amorphous phase formation at this annealing temperature. Previous studies show that the Ni atom is much faster than the Ti atom and diffuses in an immobile Ti layer matrix forming an amorphous phase [32]. Therefore, amorphization in the case of the sample annealed at 400 °C is mainly due to diffusion of one element into another. The faster diffusion of Ni atoms at this lower annealing temperature is the main cause of SSA at the interface in such ML systems.

XRD pattern at 500 °C annealing temperature of all multilayers again shows interesting structural transformation from amorphous to recrystallization due to formation of different Ti–Ni metallic phases. At this temperature, the crystallization process generally tends to occur during thermal annealing of amorphous films to get stable phases of Ti–Ni alloys, because crystalline phases are more thermodynamically favorable than the relatively low temperature formed metastable phase. In addition to this, there must be a dominant moving species,

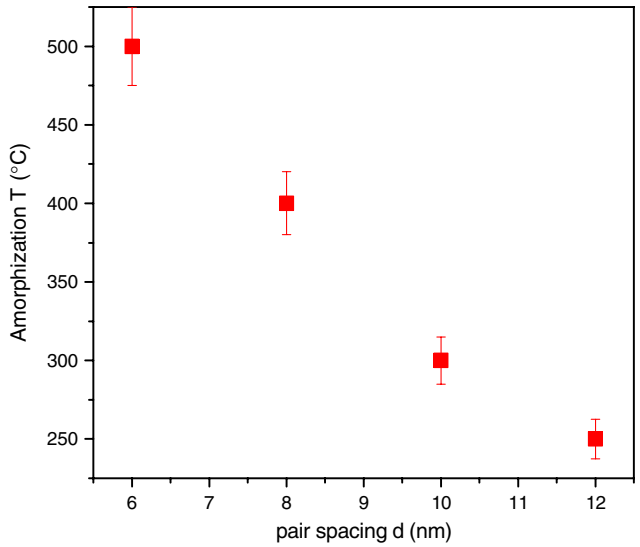

Figure 2. Trends of amorphization temperature (T_A) with multilayer pair spacing (d).

i.e. one constituent of the diffusion couple should exhibit much greater mobility than the others. The movement of both constituents is apparently required to nucleate and grow crystalline material, while mobility of only one constituent is required to grow the amorphous alloy. Such disparity in mobility of atoms in the diffusion couples provides a constraint on the formation of equilibrium intermetallic compounds in a given temperature range and time frame, i.e. kinetic constants. It has also been indicated that initially, in as-prepared composite, a certain degree of disorder present at the interface between the polycrystalline metals (if not an amorphous interfacial region) facilitates the growth of amorphous materials. Without such existing disorder at the interface, nucleation and growth of equilibrium intermetallic compounds may be favored.

By increasing the Ti layer thickness, it is clear from XRD figures that T_A decreases from 400 to 300 °C for ML B and 250 °C for ML C, as seen in figures 1(b) and (c), where we see broad humps at these temperatures. The reason for this could be connected with the ML pair spacing d, which is the sum of each individual layer thickness. For MLs A, B, and C the pair spacing d is 80 Å, 100 Å and 120 Å respectively. A decrease in amorphization temperature to values of 250 °C is found as the pair spacing increases to 120 Å as seen from figure 2. Recall that for lower d values the MLs are coherent with an ordered interfacial structure, whereas the loss of coherence or order through the growth direction progresses in samples as d increases above a certain thickness, resulting in a decrease in T_A to values as low as 250 °C. The spread in T_A, at each nominal d, is likely attributable to real differences between samples and the extent of interfacial disorder. The change in T_A with total pair spacing has also been studied and discussed previously by Jankowski *et al* in their study of SSA in Ti/Ni ML [33].

The other reason which contributes to the spread of amorphization temperature is the diffusion rate of Ni and Ti atoms with thickness variation. It is well known that in the Ti/Ni multilayer system Ni diffuses faster into immobile Ti lattices at a relatively lower annealing temperature (up to 300–400 °C). This is because of its higher mobility compared to the Ti atom. Our XPS experimental results on interfacial electronic structure of the annealed Ti/Ni multilayer also confirm strong Ni diffusion compared to the Ti atom. However, no one can ignore the possibility of Ti diffusion in the Ni layer, even though Ni has a higher diffusion rate. So considering this possibility we calculated the diffusion length for both Ti and Ni atoms in

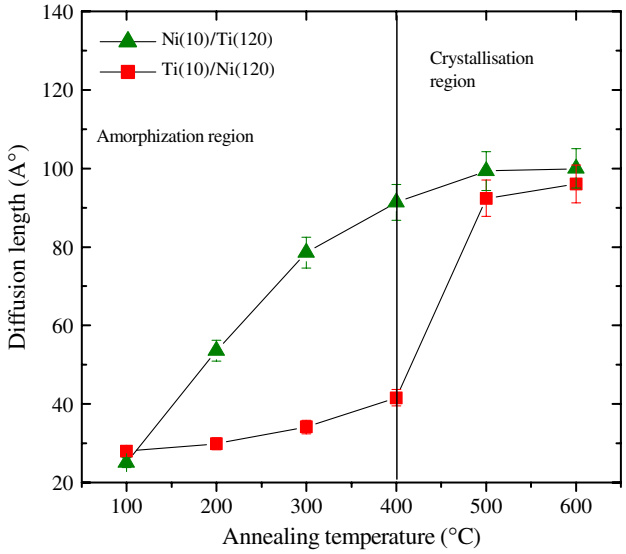

Figure 3. Diffusion length of Ti and Ni atoms in Ti/Ni and Ni/Ti bilayer film with respect to temperature.

the Ti/Ni bilayer film with respect to annealing temperatures and present it in figure 3. From this figure, it has been found that Ni has a diffusion rate higher than the Ti atom at relatively low temperatures of annealing. The trend of diffusion length for both Ti and Ni remains constant up to amorphization temperatures, whereas in the crystalline region or at high temperature annealing temperature the diffusion rate for the Ti atom increases drastically and becomes almost equal to the Ni atom's diffusion rate. Hence, a strong possibility is the diffusion of Ni atoms into Ti layers compared to Ti atoms into Ni layers at lower temperatures of annealing or up to amorphization temperature. Thus the higher diffusion length of Ni atoms with Ti layer thickness variation in the Ti/Ni multilayer makes a favorable composition (50–50%) faster for MLs having higher Ti layer thickness compared to lower Ti layer thickness MLs, and henceforth T_A decreases. It has been reported that Ti 50 at.%–Ni 50 at.% is the approximate composition for solid state amorphization to occur [34], which has also been recently confirmed by our XPS results [22].

In order to see the effect of Ti layer thickness on Ni diffusion in a multilayer system, experimentally recorded GIRXX patterns (figure not shown) were used to calculate the diffusion coefficient and diffusion length. The observed decay of the Bragg peak intensity is used to calculate the interdiffusion length in the ML using the expression [35, 36]

$$\ln[I(T)/I_0] = -8\pi^2 n^2 D(T) t/d^2$$

where I_0 is the intensity of the nth order Bragg peak at annealing time $t = 0$; $D(T)$ is the diffusivity at annealing temperature T and d is the bilayer periodicity. The diffusivities were derived from the intensity of the first order Bragg peak. The diffusivities range between 10^{-18} and 10^{-20} m^2 s^{-1}, which correspond to diffusion lengths L_d between 800 and 100 Å for annealing time (1 h) related to the diffusivity $D(T)$ through the relation

$$L_d = [2D(T)t]^{1/2}.$$

The interdiffusion coefficient is thus evaluated as a function of reciprocal temperature between 200 and 500 °C and is plotted in figure 4. Its observed trends follow an Arrhenius-type

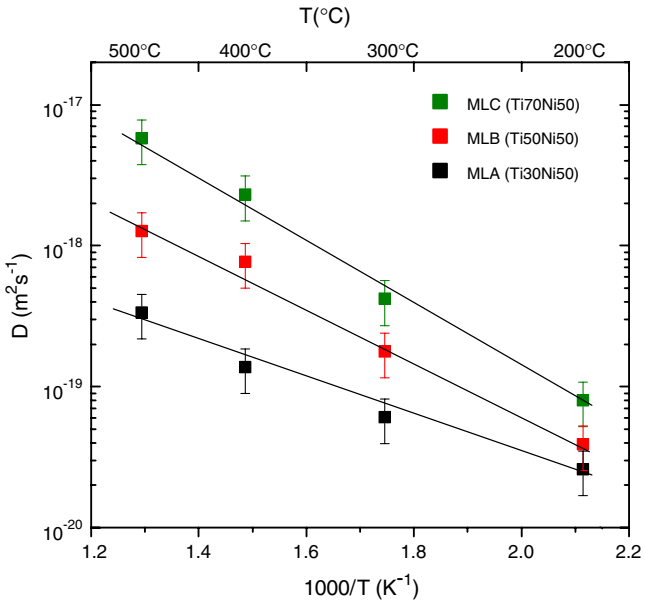

Figure 4. Interdiffusion coefficient (Arrhenius plot) of three different ML samples as a function of annealing temperature.

temperature dependence of $D(T)$, which can be expressed as

$$D(T) = D_0 \exp(-q/k_B T)$$

where q is the activation energy and k_B is the Boltzmann constant. From the interdiffusion coefficient data presented in figure 4, it can be seen that L_d increases at a much faster rate for the $d = 120$ Å ML films as compared to $d = 100$ and 80 Å ML films. The diffusion coefficients are different for each multilayer because of different activation energies as calculated by using the slope of the $D(T)$ plots. This trend appears monotonic. At the annealing temperatures where the amorphization process takes place for each ML sample A, B or C, the interdiffusion length increases rapidly. This kind of increment in L_d may be due to completion of the SSA reaction where the mobile Ni atom reacts with the Ti matrix and forms Ti–Ni alloy.

The interdiffusion coefficients of ML samples A–C at 300 °C temperature are 6.7×10^{-20}, 1.9×10^{-19} and 4.1×10^{-19} respectively. The order of magnitude difference in interdiffusion coefficients with Ti thickness at 300 °C temperature suggests a significant amount of Ni diffusion into Ti layers. This is why multilayer samples B and C exhibit SSA at this annealing temperature while sample A remains crystalline. This result suggests that atoms diffuse along the Ti/Ni interface and/or the grain boundaries of the Ti/Ni multilayer.

A common idea behind all SSA processes is that the atomic disorder created at the crystalline lattice can induce volume change and elastic softening of the lattice [37]. The strong effect of static atomic displacements inducing lattice softening as compared to thermal vibrations suggests that SSA can be regarded as a disorder induced melting process.

A similar result of solid state reaction leading to amorphization has been explained on the basis of the molecular dynamics model by Jankowski *et al* [33]. In this model, complete crystalline disorder (or amorphization) is described by the corresponding decrease in the structure factor from unity to zero with increasing temperature. The structure factor is computed as the Fourier transform of the density in each crystallographic plane parallel to the

Table 1. Coercivity H_c and saturation magnetization M_s of three different multilayer samples with annealing temperature.

	Multilayer					
	A = [Ti(30 Å)/Ni(50 Å)] × 10		B = [Ti(50 Å)/Ni(50 Å)] × 10		C = [Ti(70 Å)/Ni(50 Å)] × 10	
	H_c (Oe)	M_s (Oe)	H_c (Oe)	M_s (Oe)	H_c (Oe)	M_s (Oe)
As deposited	57.7	247.9	32.1	236.1	22.6	212.5
100 °C	27.7	252	35	225.4	16	217.8
200 °C	27	383	27	300	23	306.4
300 °C	11	No saturation	11	306		Non-magnetic
400 °C	45	No saturation	75	No saturation		Non-magnetic
500 °C		Non-magnetic		Non-magnetic		Non magnetic

interface. A Lennard-Jones molecular dynamics simulation is implemented to model the atomic arrangement of an A/B superlattice wherein A and B differ significantly in size. The simulation shows that as the temperature increases interface amorphization develops while the layer bulk remains periodic. Upon further increase in temperature, the disorder spreads to the layer bulk that is towards the center of each layer. The temperature of disorder is additionally found to scale with the layer size. The use of the structure factor to describe disorder in the molecular dynamics simulation of SSA helps to explain why amorphization temperature is increased or decreased with Ti layer thickness variations.

4. Magnetic properties

Magnetic measurements for annealed multilayer samples A, B and C are recorded using the MOKE technique and presented in figure 5. For the as-deposited case of ML sample A, measured coercivity and saturation magnetic field are 57 Oe and 247 Oe respectively. With increase in Ti layer thickness 30–50 Å, the coercivity and saturation magnetization decrease, and continue decreasing further for Ti layer thickness of 70 Å also. In this case the observed coercivity and magnetic field are 22 Oe and 100 Oe respectively. These observed thickness-dependent changes in coercivity and saturation magnetization for as-deposited multilayer films may be attributed to interdiffusion and intermixing of Ti and Ni atoms leading to non-magnetic Ti–Ni alloy phase formation at interfaces. Ti–Ni alloy phase formation at interfaces affects various parameters which are responsible for lower H_c. These parameters are (1) decreased surface roughness by interdiffusion at the interfaces of Ti and Ni multilayers; (2) enhancement of composition gradient and (3) reaction compound (solid solution of TiNi, Ti3Ni, Ti2Ni etc) at the interface of Ti and Ni. After having the Ti–Ni layer at interface the bi-layer multilayer structure converted to Ni/Ni–Ti/Ti tri-layer structures, where only Ni layers are magnetic. Coercivity and saturation magnetization with Ti layer thickness and annealing temperature up to 500 °C are summarized in table 1.

Form hysteresis loops presented in figure 5, one can see different loop shapes of multilayer samples with annealing temperature. The change in shape of the hysteresis loop with the annealing temperature can be related to the superparamagnetic contributions, where the Ni magnetic grain sizes may affect sample magnetic properties as annealing and amorphization proceeds. However, this possibility could be ruled out because of the calculated Ni grain size from the XRD patterns, which increases with thermal annealing subsequently from 42

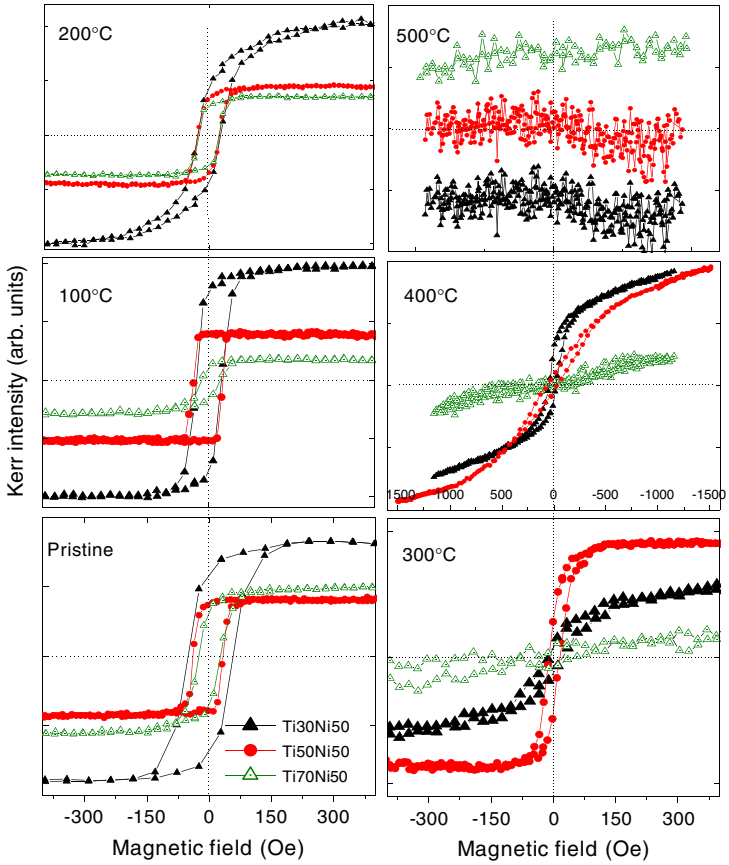

Figure 5. MOKE hysteresis loop of ML samples with different layer thicknesses and annealing temperatures.

to 190 Å at 500 °C annealing temperature [38]. For all as-prepared ML films, a square nature of the hysteresis loop is recorded, suggesting complete domain wall motion of the magnetic Ni atoms with applied magnetic field. Modifications in the shape of the hysteresis loops are seen upon annealing, where the nature of the hysteresis loops suggests a more gradual response of the domain walls and domain rotation with applied magnetic field. With further continuous annealing up to 300 °C the magnetic response drastically changed and samples started to become non-magnetic at this stage. The modification in observed magnetization behavior at this stage upon annealing may be related to significant changes in the microstructure. Ti and Ni layers convert into mixed layers consisting of ferromagnetic Ni grains separated by non-magnetic Ti grain boundaries. Formation of such a mixed layer, especially at the interface, is in agreement with the XRD data, where the Ni atoms diffuse into the Ti layers, resulting in SSA at this annealing temperature. The interdiffusion length of the Ni atoms increase both for annealing temperature and Ti layer thickness suggests the magnetic response of multilayer C should go away faster than samples B and A with temperature due to the preferred fast formation of non-magnetic Ti–Ni alloy in the case of multilayer film C. Therefore, the hysteresis loop of multilayer sample C annealed at 250 °C shows non-magnetized behavior. However, the hysteresis loop of multilayer sample A annealed at 300 °C still shows magnetization behavior Modifications in the loop shape as well as

decreased coercivity (H_c) and saturation magnetization suggest a weak magnetic response at this temperature compared to the previous or as-deposited case.

At 400°C annealing temperature, multilayer samples A and B started behaving as non-magnetic multilayers, as indicated by the nature of the recorded hysteresis loop, whereas multilayer C is completely non-magnetic at this annealing temperature. MOKE loops for multilayer samples A and B do not show any saturation up to the maximum applied magnetic field of 1500 Oe at this temperature. Corresponding GIXRR analysis of multilayer sample B provides information about a 33.5 Å-thick Ti–Ni alloy layer which is formed at the interface with reduction of Ni layer thickness from 50 to 21 Å as the ML sample undergoes SSA at this temperature. Hence, based on structural and magnetic data, we concluded that as-deposited ML stacks are converted into a Ti/Ti–Ni/Ni tri-layer structure at the amorphization temperature. It has been reported that the Ti–Ni phase is non-magnetic in nature [23], therefore the samples start to show non-magnetic nature with annealing temperature because of Ti–Ni alloy phase formation. On the other hand, in our previous work we observed Ni 3d valence band filling due to the charge transfer from the Ti to the Ni atom during the formation of Ti–Ni alloy, which is responsible for magnetism in Ti/Ni ML [22]. Indeed, hysteresis loops at 400 °C still show a weak magnetic response for samples A and B. The observed magnetic response might also be caused by the thin remaining layer (30 Å for A and 21 Å for multilayer B) of non-reacted Ni atoms, which would be present in a pure metallic form in the ML. This amount of Ni is completely converted into Ti–Ni alloy at a higher temperature of annealing at 500 °C, where all ML samples A–C show completely non-magnetic nature, as seen from figure 5. In addition to this, anisotropy is also induced with Ti layer variations and diminishes with annealing. However, the possible reason for and nature of the anisotropy, whether it is uniaxial or perpendicular anisotropy, are still not clear.

5. Conclusion

Structural results from XRD measurements show that all multilayer samples are crystalline in nature except that Ti is deposited with amorphous nature for a lower Ti layer thickness of 30 Å. Solid state amorphization is observed for each multilayer having Ti layer thickness variation with annealing treatment. It has been noticed that only one moving species is required (the Ni atom) to nucleate the solid state reaction leading to amorphization, while movement of both constituents is apparently required to grow the crystalline phase. The multilayer sample shows again recrystallization at higher temperature of annealing because of movement of both constituents to form metallic phases of Ti–Ni alloy. On the other hand, with variation in Ti layer thickness, the amorphization temperature decreases to 250 °C for multilayer sample C from 400 °C of multilayer sample A because of the different diffusion rate of Ni and multilayer pair thickness. The corresponding magnetic properties suggest that MLs start behaving non-magnetically from their amorphization temperature and completely non-magnetically at the recrystallization temperature due to the formation of a different phase of non-magnetic Ti–Ni alloy. The coercivity and magnetization values also decreased with annealing as well as with Ti layer thickness.

Acknowledgments

The authors would like to thank Dr V R Reddy and Mr S Bhardwaj for MOKE and XRD measurements respectively. In general, research by the group at Linköping University is supported by the Swedish Research Council (VR), the Swedish Foundation for Strategic

Research funded Center for Organic Electronics, COE@COIN, and the Center for Advanced Molecular Materials, CAMM.

References

[1] Falicov L M, Pierce D T, Bader S D, Gronsky R, Hathaway K B, Hopster H J, Lambeth D N, Parkin S S P, Prinz G, Salamon M, Schuller I K and Victora R H 1990 *J. Mater. Res.* **5** 1299
[2] Schuller I K, Kim S and Leighton C 1999 *J. Magn. Magn. Mater.* **200** 571
[3] Okawa N, Tanaka H, Akiyama R, Matsumoto T and Kawai T 2000 *Solid State Commun.* **114** 601
[4] Haghiri-Gosnet A M, Wolfman J, Mercey B, Simon Ch, Lecoeur P, Korzenski M and Hervieu M 2000 *J. Appl. Phys.* **88** 4257
[5] Mathwsa M, Postma F M, Lodder J C and Jansen R 2005 *Appl. Phys. Lett.* **87** 242407
[6] Jeon H J, Kim I, Kim J, Kim K H and Yamaguchi M 2004 *J. Magn. Magn. Mater.* **272–276** 382–4
[7] Kim Y M, Hen S H, Kim H J, Choi D, Kim K H and Kim J 2002 *J. Appl. Phys.* **91** 8462
[8] Kim K H, Kim Y H, Kim J, Han S H and Kim H J 2000 *J. Magn. Magn. Mater.* **215/216** 428
[9] Xiong C M, Sun J R and Shen B G 2005 *Solid State Commun.* **134** 465–9
[10] Ishida A and Sato M 2003 *Acta Mater.* **51** 5571–8
[11] Castaño F J, Stobiecki T, Gibbs M R J, Czapkiewicz M, Wrona J and Kopcewicz M 1999 *Thin Solid Films* **348** 233–7
[12] Katsuki F, Hanafusa K, Yonemura M, Koyama T and Doi M 2001 *J. Appl. Phys.* **89** 4643
[13] Yan H F, Shen Y X, Guo H B and Liu B X 2007 *J. Phys.: Condens. Matter* **19** 026219
[14] Concustell A, Mattern N, Wendrock H, Kuehn U, Gebert A, Eckert J, Greer A L, Sort J and Baro M D 2007 *Scr. Mater.* **56** 85
[15] Schwarz R B and Johnson W L 1983 *Phys. Rev. Lett.* **51** 415
[16] Johnson W L 1986 *Prog. Mater. Sci.* **30** 81
[17] Schwarz R B 1988 *Mater. Sci. Eng.* **97** 71
[18] Clemens B M 1986 *Phys. Rev.* B **33** 7615
[19] Clemens B M 1987 *J. Appl. Phys.* **61** 4525
[20] Lehnert T, Grimmer H, Böni P, Horisberger M and Gotthardt R 2000 *Acta Mater.* **48** 4065
[21] Vedpathak M, Basu S, Gokhale S and Kulkarni S K 1998 *Thin Solid Films* **335** 13–8
[22] Bhatt P and Chaudhari S M 2005 *J. Phys.: Condens. Matter* **17** 7465
[23] Bhatt P, Sharma A and Chaudhari S M 2005 *J. Appl. Phys.* **97** 043509
[24] Lee1 Y P, Kim K W, Kudryavtsev Y V, Nemoshkalenko V V and Szymanski B 2002 *Eur. Phys. J.* B **26** 41
[25] Kudryavtsev Y V, Nemoshkalenko V V, Lee Y P, Kim K W, Kim C G and Szymanski B 2000 *J. Appl. Phys.* **88** 2430
[26] Saito K and Iwaki M 1884 *J. Appl. Phys.* **55** 4447
[27] Vredenberg A M, Westendorp J F M, Saris F W, van den Pers N M and de Kedser T H 1986 *J. Mater. Res.* **1** 774
[28] Chaudhari S M, Suresh N, Phase D M, Gupta A and Dasannacharya B A 1999 *J. Vac. Sci. Technol.* A **17** 242
[29] Gupta R, Gupta M, Kulkarni S K, Kharrazi S, Gupta A and Chaudhari S M 2006 *Thin Solid Film* **515** 2213–9
[30] Warren B E 1969 *X-ray Diffraction* (Reading, MA: Addison-Wesely)
[31] Hollanders M A, Thijsse B J and Mittemeijer E J 1990 *Phys. Rev.* B **42** 5481
[32] Lehnert T, Tixier S, Böni P and Gotthardt R 1999 *Mater. Sci. Eng.* A **273** 713
[33] Jankowski A F, Sandoval P and Hayes J P 1995 *Nanostruct. Mater.* **5** 497
[34] Thoma A 1990 *J. Phys.: Condens. Matter* **2** 3167
[35] Mizoguchi T and Murata M 1991 *Japan. J. Appl. Phys.* **30** 1818
[36] Speakmann J, Rose P, Hunt J A, Cowlam N, Somekh R E and Greer A L 1996 *J. Magn. Magn. Mater.* **156** 411
[37] Lam N Q and Okamoto P R 1994 *Mater. Res. Sot. Bull.* **19** 41
[38] Bhatt P, Ganeshan V, Reddy V R and Chaudhari S M 2006 *Appl. Surf. Sci.* **253** 2572